

Observations of Toroidal Coupling for Low- n Alfvén Modes in the TCA Tokamak

K. Appert, G. A. Collins, F. Hofmann, R. Keller, A. Lietti, J. B. Lister, A. Pochelon, and L. Villard

Centre de Recherches en Physique des Plasmas, Association Euratom–Confédération Suisse, Ecole Polytechnique Fédérale de Lausanne, CH-1007 Lausanne, Switzerland

(Received 21 November 1984)

The antenna structure in the TCA tokamak is phased to excite preferentially Alfvén waves with known toroidal and poloidal wave numbers. Surprisingly, the loading spectrum includes both discrete and continuum modes with poloidal wave numbers incompatible with the antenna phasing. These additional modes, which are important for our heating experiments, can be attributed to linear mode coupling induced by the toroidicity of the plasma column, when we take into account ion-cyclotron effects.

PACS numbers: 52.40.Db, 52.50.Gj, 52.55.Fa

Although the particular geometry of a tokamak is known to be important when considering the excitation of radio-frequency waves for additional heating of the plasma, there are almost no direct experimental observations which can be attributed to toroidicity. Alfvén-wave heating, currently being studied on several tokamaks,¹⁻⁵ is characterized by low toroidal wave numbers ($n=1-4$) and frequencies less than the ion-cyclotron frequency ($\omega < \omega_{ci}$) and has been predicted to be especially sensitive to the toroidal geometry. We report in this Letter on experimental observations which can only be explained by toroidicity, although they were not previously predicted theoretically, and also on observations which are compatible with earlier calculations.^{6,7} The inclusion of ion-cyclotron effects in the theoretical model has given a better representation of the experiment.

The experiments have been carried out in the TCA tokamak with major radius $R=0.61$ m, minor radius $a=0.18$ m, and toroidal magnetic field $B_\phi=1.5$ T. A plasma current of 130 kA gives the safety factor at the limiter radius $q(a)\sim 3.2$, an electron temperature $T_e\sim 800$ eV, and an effective charge $Z_{\text{eff}}\sim 3$. The antenna structure consists of eight groups of six 10-mm-diam bars sited at four different toroidal locations above and below the plasma, 30 mm behind the limiter radius. Each group is fed separately so that the dominant toroidal (n) and poloidal (m) wave numbers can be determined by their relative phasings. The usual case is $N=2$, $M=1$ which contains $n=\pm 2, \pm 6, \dots$, $m=\pm 1, \pm 3, \dots$ in the excitation structure. The generator frequency of 2.5 MHz gives $\omega/\omega_{ci}=0.22$ for a deuterium plasma and the spectrum is scanned by increasing the plasma density.

The antenna is designed to excite a compressional or fast magnetosonic wave which converts to the kinetic Alfvén wave at a radius r_0 defined by the Alfvén resonance condition, given in the large-aspect-ratio approximation by

$$\frac{n+m/q(r_0)}{R} = k_A(r_0) = \frac{\omega(1-\omega^2/\omega_{ci}^2)^{-1/2}}{V_A(r_0)}, \quad (1)$$

where $V_A(r) = B_\phi[\mu_0\rho(r)]^{1/2}$ represents the local Alfvén velocity and $\rho(r)$ the profile of mass density. The resonance condition itself can be altered in a tokamak,⁸ but only at very low plasma densities ($\bar{n}_e \sim 1 \times 10^{12} \text{ cm}^{-3}$) would such an effect be expected.

Equation (1) defines a resonance layer from which the kinetic Alfvén wave propagates toward the interior of the plasma and is subsequently damped, heating the particles.⁹ As the plasma density increases the resonance layer moves through the plasma and a broad continuum is seen in the antenna loading spectrum. Global eigenmodes of the shear Alfvén wave can be excited at a frequency just below the threshold of the continuum defined by Eq. (1). The excitation of this wave, which is often called the discrete Alfvén wave (DAW), appears as a peak in the loading spectrum.

In Figs. 1(a) and 1(b) measurements of the antenna loading as a function of the line-averaged electron density, made in the standard conditions, are compared with a cylindrical magnetohydrodynamical (MHD) calculation that includes ion-cyclotron effects. To enable comparison with spectra obtained with other gases or at different toroidal fields, a global Alfvén wave number k_A^* has been introduced. This is defined by Eq. (1) with use of the line-averaged electron density and an effective ionic mass of 2.0 for deuterium and 1.3 for hydrogen.¹⁰ In the large-aspect-ratio approximation the principal modes resonant with the antenna excitation structure are the $(n,m)=(2,-1)$ and $(-2,1)$ continua with a very low density threshold, the $(2,1)$ and $(-2,-1)$ continua with their threshold near $\bar{n}_e \sim 4 \times 10^{13} \text{ cm}^{-3}$, and the $(-2,-1)$ and $(2,1)$ DAW's just below this latter threshold. Although modes with the same helicity (i.e., n/m positive or negative) are degenerate in the context of ideal MHD, modes with $m=-1$ are observed to be preferentially excited¹¹ because of ion-cyclotron effects on the compressional waves excited by the antenna. In our case these are the so-called "surface" waves which are known to have their eigenfrequencies slightly above the threshold of the corresponding continuum if $m < 0$.¹²

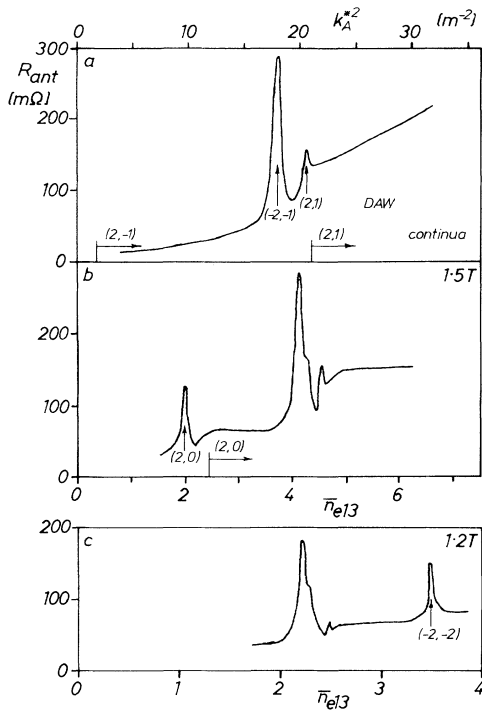


FIG. 1. Loading per antenna group as a function of line-averaged electron density ($N=2$, $M=1$, deuterium plasma). (a) Cylindrical calculation; (b) measurements in standard conditions; (c) measurements at lower toroidal field and with side shields.

While the main features of the measurements in Fig. 1(b) are attributable to the $n = \pm 2$, $m = \pm 1$ modes which dominate the $N=2$, $M=1$ antenna excitation structure, the most obvious discrepancy with the cylindrical calculations is the appearance of a mode, both DAW and subsequent continuum, near $\bar{n}_e \sim 2 \times 10^{13} \text{ cm}^{-3}$ at the estimated threshold of the $(\pm 2, 0)$ continua. To study this region of the spectrum in detail we have used a hydrogen plasma and in Fig. 2 we compare the loading due to various antenna structures. The possibility that parasitic components in the excitation structure may be responsible for the new mode was considered but careful attention to balancing the amplitude and phase of the antenna currents has resulted in a spectral purity greater than the measurement sensitivity. The $(-1, -1)$ DAW is not excited by an $N=2$, $M=1$ phasing (Fig. 2), nor is the $(-2, -1)$ DAW excited by an $N=1$, $M=1$ phasing, demonstrating the purity of toroidal mode numbers. Similarly the $(-2, -1)$ and $(-1, -1)$ DAW's are not excited by the $N=2$, $M=0$ or $N=1$, $M=0$ phasings, demonstrating the purity of poloidal mode numbers. In Fig. 2 the new DAW at $\bar{n}_e \sim 3.2 \times 10^{13} \text{ cm}^{-3}$ is clearly distinct from the $(-1, -1)$ DAW at $2.3 \times 10^{13} \text{ cm}^{-3}$, an observation which was particularly

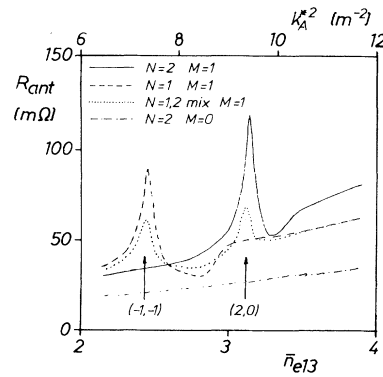


FIG. 2. Loading near the $(2,0)$ threshold measured for different antenna phasings (hydrogen plasma).

obvious when we used an antenna phasing that produced an equal mixture of $N=1$ and $N=2$. We identify the new mode as $n=2$, $m=0$ both by its position in the spectrum and from the relative amplitudes of the vacuum magnetic field components of the DAW, the latter measured by a probe inserted above the plasma. A probe inserted equatorially showed a more complicated poloidal structure. Surprisingly an $N=2$ $M=0$ antenna did not excite the new mode. That is, however, consistent with the lack of an $m=0$ compressional wave in our experimental range so that an $M=0$ antenna can only have very weak coupling to the plasma.

Toroidal coupling is the evident candidate for excitation of the $(2,0)$ mode by a $(2, -1)$ compressional wave since there exist several effects for coupling the principal mode with poloidal wave number m to other modes with wave numbers $m \pm 1$.¹³ The dominant of these effects is the poloidal variation of the toroidal field on a magnetic surface; although the curvature inherent in toroidal geometry, variations from symmetry in the poloidal plane (such as displacement of the plasma column), and distortion of the antenna current distribution also contribute to this mode mixing. Even though in toroidal geometry the modes are no longer pure harmonics of the poloidal angle we continue to use as a label the m number for the corresponding cylindrical mode, which remains the most important component. Our model takes fully into account both the toroidal geometry and ion-cyclotron effects and uses the same numerical method as outlined in Ref. 6. For a single-helicity $(2, -1)$ antenna we obtain the result shown in Fig. 3. Despite the numerical uncertainty we see a well-defined peak in the loading spectrum close to the position of the experimentally observed peak. This DAW has dominantly $m=0$ behavior at the interior of the plasma but a more complicated poloidal structure near the edge due to higher- m resonance layers. The same model in the

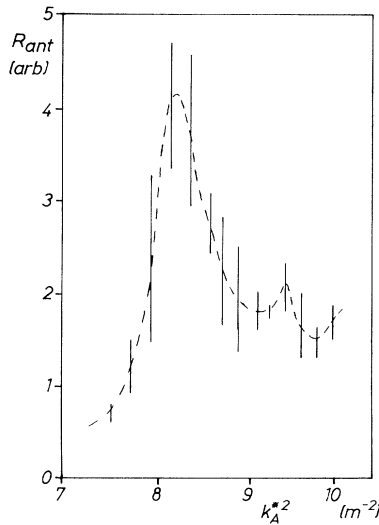


FIG. 3. Loading near the (2,0) threshold calculated with use of the complete toroidal model for a single-helicity (2, -1) antenna.

ideal MHD limit ($\omega/\omega_{ci}=0$) showed no clear peak. We also found that, in agreement with the experiment, a (2,0) antenna coupled very weakly to the plasma and no DAW peak appeared.

The presence of high- m surfaces, as mentioned above, makes it difficult to assess the importance of the $m=0$ continuum. However, their effect is exaggerated in the numerical calculations by the use of an antenna current distribution expressed as a harmonic of the poloidal angle. Although this corresponds to an ideal cylindrical antenna, a more realistic model of the TCA antenna and its current distribution gives quite acceptable energy deposition at the $m=0$ resonance layer when it is near the center of the plasma, as well as an antenna loading comparable with that seen in the experiment. In Fig. 4 we present profiles of energy flux above and below the (2,0) threshold, calculated with the assumption that dissipation is localized at the resonance layer (e.g., resistive damping). It is known that this gives a reasonable estimate of the energy that is deposited at each layer, even though it does not correctly model the dissipation of the kinetic Alfvén wave.⁹ Also shown in Fig. 4 is the energy deposition profile for a $M=0$ antenna.

Having confirmed the importance of toroidal coupling, we reconsidered an earlier prediction⁷ of toroidal coupling to the (-2, -2) mode when (-2, -1) is the principal directly excited mode. To explore this region we lowered the toroidal field to $B_\phi=1.2$ T, keeping $q(a) \sim 3.2$. As shown in Fig. 1(c) a DAW is observed near the (-2, -2) threshold at $\bar{n}_e \sim 3.5 \times 10^{13}$ this peak is almost coincident with the (-3, -1) DAW [see Eq. (1)] which can be directly excited from an $N=1, M=1$ antenna structure. At lower values of

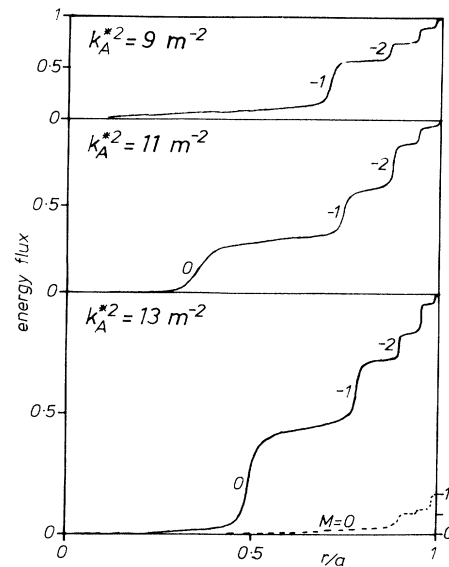


FIG. 4. Profiles of energy flux above and below the (2,0) threshold as calculated by the toroidal model (in the ideal MHD limit) for TCA geometry and $N=2, M=1$ antenna phasing. The total absorbed energy is shown scaled to the antenna resistance which increases when the $m=0$ layer appears in the plasma.

the plasma current the two peaks separated. In Fig. 5 it can be seen that both the general form of the loading resonance and its modulation by q -profile fluctuations at the sawtooth frequency¹⁴ distinguish the (-2, -2)

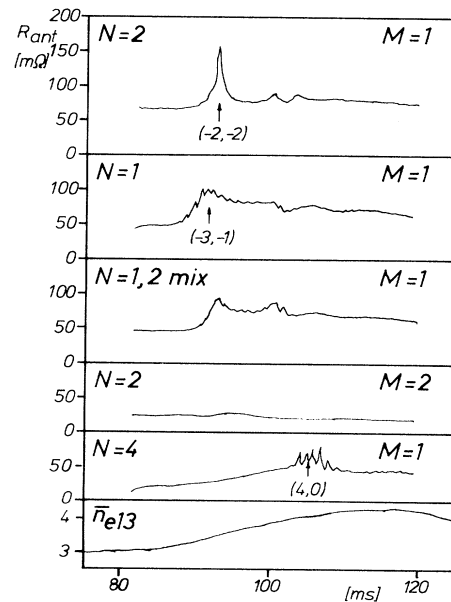


FIG. 5. Loading near the (-2, -2) DAW measured for different antenna phasings by increasing the electron density during each shot ($B_\phi=1.2$ T, deuterium plasma, with side shields).

DAW excited by the $N=2$, $M=1$ antenna from the $(-3, -1)$ DAW. Direct excitation of the $(-2, -2)$ DAW by an $N=2$, $M=2$ antenna is not observed, consistent with calculation. To complete the study of this region of the spectrum we also show in Fig. 5 the excitation of the $(4,0)$ mode by the $N=4$, $M=1$ antenna and take this as further evidence of toroidal coupling, analogous to the case of $(2,0)$.

In conclusion, we are confident that we have observed the excitation of modes with poloidal wave numbers incompatible with the antenna phasing and that they can be accounted for by toroidal coupling with the inclusion of ion-cyclotron effects. In each case the toroidally coupled mode has an m number which differs by 1 from the principal directly excited mode and provides a means for energy to be deposited closer to the center of the plasma. Direct excitation of these additional modes is difficult since the experimental conditions are such that compressional waves with these poloidal wave numbers are only weakly excited by the antenna. The $(2,0)$ mode has particular importance for our heating experiments in that it is in the region of the spectrum where the best electron and ion heating have been seen, but where a cylindrical calculation would suggest that the excited resonance layers are far from the plasma center, and in that crossing the $(2,0)$ continuum threshold during rf heating often has a dramatic effect on the plasma.¹

We acknowledge the interest of Professor F. Troyon and the support of all our technical staff. The work

described here was partially supported by the Swiss National Science Foundation.

¹R. Behn *et al.*, Plasma Phys. Contr. Fusion **26**, 173 (1984).

²F. D. Witherspoon, S. C. Prager, and J. C. Sprott, Phys. Rev. Lett. **53**, 1559 (1984).

³T. E. Evans *et al.*, Phys. Rev. Lett. **53**, 1743 (1984).

⁴R. A. Demirkhanov *et al.*, in *Proceedings of the Ninth International Conference on Plasma Physics and Controlled Nuclear Fusion Research, Baltimore, 1982* (International Atomic Energy Agency, Vienna, 1983) Vol. 2, p. 91.

⁵M. H. Brennan *et al.*, in *Heating in Toroidal Plasmas* (International School of Plasma Physics, Varenna, 1984), Vol. 1, p. 153.

⁶K. Appert *et al.*, Nucl. Fusion **22**, 903 (1982).

⁷K. Appert, R. Gruber, F. Troyon, and J. Vaclavik, Plasma Phys. **24**, 1147 (1982).

⁸C. E. Kieras and J. A. Tataronis, J. Plasma Phys. **28**, 395 (1982).

⁹A. Hasegawa and L. Chen, Phys. Fluids **19**, 1924 (1976).

¹⁰A. de Chambrier *et al.*, Plasma Phys. **24**, 893 (1982).

¹¹A. de Chambrier *et al.*, Helv. Phys. Acta **57**, 110 (1984).

¹²N. F. Cramer and I. J. Donnelly, Plasma Phys. **25**, 703 (1983).

¹³A. G. Kirov *et al.*, in *Proceedings of the Tenth International Conference on Plasma Physics and Controlled Nuclear Fusion Research, London, 1984*, International Atomic Energy Agency Report No. IAEA-CN-44/F-IV-8-1 (to be published).

¹⁴A. de Chambrier *et al.*, Phys. Lett. **92A**, 279 (1982).